ADVANCED PHYSIOLOGICAL ESTIMATION OF COGNITIVE STATUS

Leonard J. Trejo, Roman Rosipal
Pacific Development and Technology, LLC
Palo Alto, CA 94303

Paul L. Nunez
Cognitive Dissonance, LLC
Covington, LA 70433

ABSTRACT

We developed new algorithms for *Advanced Physiological Estimation of Cognitive Status* (APECS), which significantly improved the estimation of cognitive workload and shed new light on the estimation of mental fatigue. More specifically, we used *atomic decomposition* to identify unique sources of brain electrical activity as measured by the EEG recorded in human participants as they performed tasks that induced different mental states, including engagement, mental workload, and mental fatigue. We tested two types of atomic decomposition, each of which identifies unique EEG sources simultaneously in three dimensions: 1) atoms with dimensions of power spectral density, space (electrode position), and time (time on task or task conditions), or 2) atoms with dimensions of magnitude squared coherence, spatial relationships (electrode pairs), and time. For tasks that induced mental workload, we found atoms that combine sources in the theta (4-8 Hz) and alpha (8-12 Hz) EEG frequency bands consistently in individual participants at different times of day and on different days. The temporal variations of the atoms clearly reflected the levels of mental workload induced by varying task conditions. For a task that induced mental fatigue, we found atoms that tracked the development of mental fatigue in individual participants over time, while reflecting underlying changes in power or coherence of primarily theta-band EEG. Our results show that atomic decomposition is a valuable new approach to the identification and measurement of EEG sources for monitoring cognitive status. By comparing these results with results of prior analyses using the same data sets, we observed that atomic decomposition can supplement or overcome existing approaches based on conventional two-dimensional space-time or frequency-time decomposition of EEG.

1. INTRODUCTION

Over the past four years, scientists at PDT have developed several advanced computational algorithms for real-time classification of mental states that can run on small hand-held computers or be embedded in the controls of vehicles, aircraft, spacecraft, and even in the helmets of foot soldiers, pilots, and astronauts. The PDT algorithms are known as APECS, which stands for Advanced Physiological Estimation of Cognitive Status, and have been rigorously tested in a series of controlled experiments sponsored by the US Army Research Office.[1,2,3] The algorithms also build on related studies from the US Air Force and NASA.[4,5] These studies have proven the accuracy of the APECS algorithms for EEG-based detection and classification of mental states including engagement, workload, and fatigue during the performance of mental work.

The APECS algorithms use proprietary implementations of cutting-edge machine learning and statistical pattern recognition, including kernel partial least squares (KPLS) and parallel factor analyses (PARAFAC). By applying these methods to massive amounts of experimental data, PDT scientists decomposed multi-sensor EEG spectra into a small set of elemental components or atoms that are important for estimating mental states. The APECS algorithms are designed to handle practically unlimited numbers of input channels and spectral resolutions. The algorithms are also highly adaptive, requiring no a priori information the spatial or spectral distributions of the atoms.

2. METHODS

Neurocognitive Databases. We have access to five databases from controlled studies of physiology and human performance, including four studies that focused on estimation of cognitive workload and detection of cognitive overload. Drs. Trejo and Rosipal directed experiments, wrote algorithms or analyzed data from each of these studies and are uniquely familiar with the databases. We used three of these databases to develop and test APECS algorithms. All data from these studies were collected with informed consent and approved IRB protocols. The data were coded such that the identities of the participants will be unknown to PDT analysts. The three databases used in the present project included:

1. USAF-C: C2ISR Multimodal Study of UAV Operator Readiness (6 multi-test participants17)
2. USA-T: Army Toxins II Multimodal Study of Cognitive Overload (8 test-retest participants4)
3. NASA-C: NASA Cognitive Fatigue Database (16 participants, public domain6)
4. USN-B: Navy Biopsychometric Assessment Program Database (8 test-retest participants)
5. NASA-E: NASA ERTAS Database (8 test-retest participants13)

2.1 Task 1. Analysis of Tasks, Workload Metrics, and Physiological Data

The aim of this task was to decompose each experimental database to define workload, time resolution, and physiological metrics. For each database, we followed a three-step process of algorithm adaptation and testing (Figure 1). First, we analyzed each task from a neuro-cognitive standpoint to guide our selection of workload and physiological metrics and time resolution. For example, the USAF-C database includes visual signal-detection, working memory, and executive control tasks. Perceptual tasks, such as signal detection, would activate visual-spatial processing networks located in occipital, parietal, and inferotemporal cortex, which will modulate alpha 1 and alpha 2 powers and coherence. The working memory demands of the USAF-C task would activate the anterior cingulate and dorsolateral prefrontal cortex, producing increased midline frontal theta rhythms.[6] This prior knowledge of functional specialization guided our selection of EEG electrode sites, frequency bands, and spatial / temporal resolution for power and coherence estimates.

The temporal resolution of EEG analysis for each task was long enough to reliably estimate parameters but short enough to detect changes related to task conditions. By applying these principles to each task, we produced a set of analysis parameters (Table 1).

2.2 Task 2. APECS-W Algorithm Adaptation

As suggested by a current theory of local/global EEG coherence**Error! Bookmark not defined.** and experiments on EEG and cognitive function,[7] we hypothesize that cognitive workload is reflected by the desynchronization of a parietal alpha atom defined by long-range coherence with frontal regions and the synchronization of a frontal midline theta atom defined by local coherence with neighboring frontal regions. Using this guiding hypothesis and the analyses from Task 1, we structured two APECS-W algorithms for each database. In the first algorithm, or APECS-Wp, aimed at power spectral density effects, the three-way input matrix consisted of EEG power spectral densities for frequency bins from 1-25 Hz, electrode position, and time of measurement (which reflected task-induced workload transitions). In the second algorithm, or APECS-Wc, aimed at spectral coherence effects, the three-way input matrix consisted of multi-scale EEG coherence spectra, electrode-pair (all unique pairs of electrodes excluding self-pairing), and time. For the NASA-C database we structure two similar algorithms, APECS-Fp and APECS-Fc, using similar principles, but different constraints (see below).

Task Code	Perceptual & Cognitive Processing Demands	Neural Sources	EEG Bandwidth	Range Of Temporal Resolution	Minimum Frequency Resolution
USAF-C	Visual signal detection Working memory & executive control	Parietal-occipital Fronto central	8-25 Hz 4-8 Hz 8-12 Hz	2-3.5 s 2-3.5s 2-8 s	1.0 Hz 1.0 Hz 0.5 Hz
USA-T	Visual signal detection Auditory language processing Working memory & executive control	Parietal-occipital Temporal-central Fronto central	8-20 Hz 8-20 Hz 4-12 Hz	2-3.5 s 2-3.5s 2-8s	1.0 Hz 1.0 Hz 1.0 Hz
NASA-C	Working memory & executive control	Fronto central	4-18 Hz	2-13 s	0.5 Hz

Table 1. Spatial, frequency, and temporal analysis parameters for the three task databases.

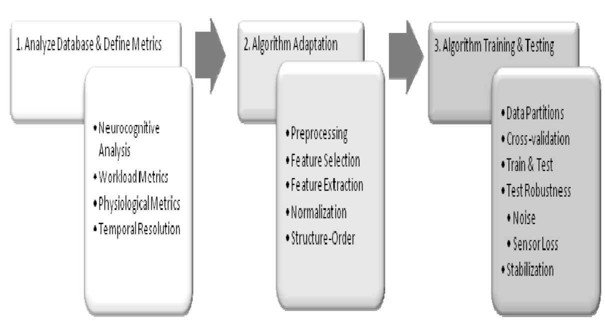

Figure 1. Three-step process of APECS-W algorithm adaptation and testing. In Step 1, we use neurocognitive theory and data to analyze tasks to define workload, time, and physiological metrics. In Step 2, we will define preprocessing, feature selection/extraction, normalization methods and adapt the APECS structure and order to the features. In Step 3 we will select random training, cross-validation, and testing partitions then train and test the algorithm. In future studies we may also test the resulting algorithm for tolerance of noise and sensor loss, and then apply optional stabilization methods to improve test-retest reliability.

In the present analyses the outputs consisted of unique atoms for which we obtained the loadings using PARAFAC decomposition with the following constraints:

- We corrected EEG records for ocular artifacts and segmented them into non-overlapping contiguous epochs of 2-s duration, providing frequency resolution of 0.5 Hz. This resolution was satisfactory for all task requirements (Table 1).
- We performed outlier detection by removing points with unduly high leverage. For this we did an initial PARAFAC decomposition and then clipped data points for which individual loadings in any one dimension exceeded a fixed percentile of the populations of loadings for that dimension in the given experiment. The percentiles we used ranged from 90 to 99%. After removing such points we did a second decomposition and retained the loadings as results.
- We imposed a constraint of non-negativity for loadings on all dimensions of the PARAFAC decompositions. In addition, for the NASA-C dataset, coherence analysis, we used an additional constraint of unimodality on the frequency dimension.
- We did not rescale or normalize data for any dimension. However, for display purposes only, we scaled loadings for the *time* dimension for comparing atoms with very different loading means and variances within experiments.
- Units of power spectral density were $dB/\sqrt{Hz}$. Units of coherence were the conventional dimensionless units of magnitude squared coherence ranging in value from 0 to 1, where 0 means no coherence and 1 means perfect coherence at a given frequency.

Two approaches were used to assign initial values to the loadings before iterating solutions to the PARAFAC decompositions. For both APECS-W algorithms we used a method of performing several small runs then averaging the resulting loadings and using the averages to initialize the loadings for complete decompositions. For the APECS-F algorithm, we used singular value decompositions in each dimension to estimate the initial loadings.

For APECS-W we used a uniform convergence criterion of 1.0×10^{-6} for iterating the algorithm, i.e., iteration ceased when the change in total variance explained was less than $1/10{,}000^{th}$ of one percent. For APECS-F the convergence criterion was 0.001 or an improvement in the model fit of less than $1/10^{th}$ of one percent.

After preprocessing all EEG records to remove EOG artifacts we performed three-way unsupervised PARAFAC decompositions to identify the atoms (multidimensional components of variance) in the three-way input matrices. For the APECS-Wp and APECS-Fp algorithms, the EEG atoms, A, are defined as three-way sources with dimensions of frequency, f, electrode, e, and time, t (Eq. 1). Each atom is estimated by two normalized vectors (a, b), a score vector c and a noise term, ε_{eft}.

$$\hat{A}_{eft} = \sum_{k=1}^{N_k} a_{ek} b_{fk} c_{tk} + \varepsilon_{eft} \qquad \text{(Eq. 1)}$$

2.3 Task 3. Algorithm Training and Testing

The structure of the APECS-W algorithm was similar for each database, but we adapted the variable inputs, outputs, and preprocessing requirements of each database to a format that was suited for cross-study validation. Since all of the decompositions we did were unsupervised, there was no need for formal training, testing, and validation sets. However, for the USAF-C and USA-T datasets we used sessions performed at different times of day and on different days for this purpose. For example, we used session data from Day 1 to estimate the atoms and then projected the EEG data for Day 2 using the weight vectors for each atom to reproduce the time course of each atom across workload conditions. No test-retest validations were performed as of yet for the NASA-C data set.

Data were collected from six participants in the USAF-C study (denoted 'B', 'C', 'E', 'G', ''I', and 'K'), each of whom completed three sessions (trial repetitions). Participants were trained to stable performance on a simulated Unmanned Air Vehicle (UAV) task. The task consisted of monitoring the progress of four UAVs as they flew a preplanned mission, monitoring UAV resources, and classifying synthetic aperture radar images acquired by sensors in each UAV. Each run contained six different indicators of mental states assigned by the experimenters; however, indicators for only two workload levels (low and high) were provided to us due to a security restriction. Therefore, we used only the data from the two periods designated as high- and low workload. Nineteen channels of EEG (placed according to the International 10-20 System with a linked mastoid reference) were available in this study. One-channel ECG and two channels of bipolar EOG (vertical and horizontal) were also recorded.

First, the EEG data were down-sampled to 128 Hz sampling rate from the original sampling rate of 256 Hz. Next, data were segmented into non-overlapping consecutive windows of 2-s duration. As in the initial analyses30 (Appendix 1), the power spectral density (PSD) was computed for each segment using the Thomson Multi-taper method. Initial analyses revealed a high level of power at frequencies below 6 Hz. Power at these frequencies often arose from motion artifacts and confounded the PARAFAC analyses of EEG. Therefore, only the frequencies in the range of 6 to 25 Hz were considered in this study. We repeated this procedure for each EEG channel separately and constructed a three-dimensional matrix, A(E × F × T), with E time segments, F electrodes and PSD estimates at T frequencies (Eq. 1).

3. RESULTS

In this project we designed and tested an APECS workload algorithm (APECS-W), to increase the accuracy and reliability of estimated cognitive workload and detect periods of cognitive overload. We aimed for a 20% increase in accuracy and test-retest reliability. Our minimally successful criterion was 10%. Our prior simulations showed that even a 10% improvement will move estimation of workload near the lower range of accuracy now possible for estimation of engagement or fatigue. We considered distinguishing engagement from workload, but our focus was on discriminating workload states pertaining to active task engagements. We tested the APECS-W algorithm using two databases (USAF-C, USA-T) described above. A formal classification analysis was outside the scope of this STIR project, so we made informal estimates of accuracy based on inspection of the data and comparisons with prior results. We will perform formal classification analyses in our future development of the APECS algorithms. For now, our experience with all of the data sets examined here suggests that there was an improvement of more than 20% in the estimation of cognitive workload using atomic decomposition, as compared to our prior methods using two-way analyses. For the fatigue data, we estimated a lower level of improvement, which is to be expected from the already-high accuracies of prior classifications.

We designed the APECS algorithm to be adaptable to a wide range of tasks that require human performance or supervision. In particular, we adapted the algorithm to the estimation of mental fatigue, and will refer to this algorithm variant as APECS-F. Although we did not set out to compare APECS-F quantitatively with prior results, we report below that APECS-F was highly successful in identifying EEG atoms that track the development of mental fatigue in individual participants. Due to space limitations, only a portion of the results are presented here; a full set appears in the corresponding poster.

The PARAFAC model has been run two times. After the convergence of the first run the points with high values of the residual variance and leverage, that is, points indicating noisy samples, were inspecting. The points exceeding 95 percentile of the residual variance and leverage distribution were removed and the PARAFAC model was run again. In general, this procedure removed points with very high values of temporal loadings (signatures). The core consistency10 of these final models was in all cases greater than 85% indicating a good model fit.

First, the PARAFAC model was run using the full set of 19 EEG electrodes. The results of the three-atom PARAFAC model for Participant B are depicted in (Figure 2). It can be observed that the temporal signatures of the second and third atoms separate the periods of the high and low workload. However, high values of the loadings vectors at frequencies above 20 Hz indicate that this can be due to the movement components superimposed to EEG. To investigate this effect the spatial loading vectors for Atom 2 and 3 are plotted in Figure 3.

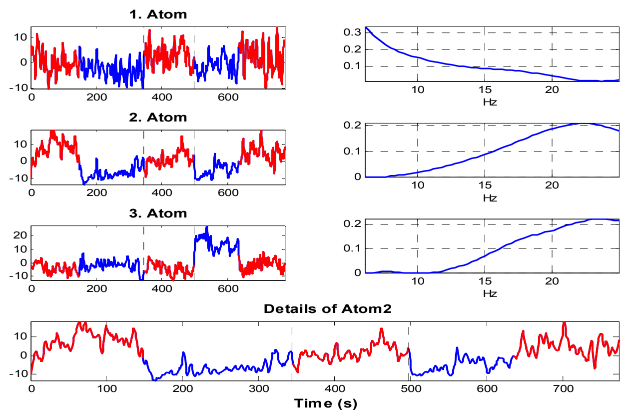

Figure 2. Loadings of three PARAFAC atoms extracted from EEG recordings of Participant B using 19 electrodes. Left panel: Temporal signatures of the EEG atoms. Red marks indicate periods of high workload, blue line marks the low workload periods. Vertical dotted lines separate three distinct experimental sessions. Bottom panel: Detailed plot of temporal loadings of Atom 2. Right panel: Spectral signatures corresponding to atoms numbered in the left panel.

High spatial loading values can be observed at T3, T4, F7 and Fp2 sites (Atom 2) and at the electrode sites Fp1, Fp2, T5, T6 and F7 for Atom 3. These electrodes are generally known to be susceptible to the movement artifact. Therefore in the next step we have removed these electrodes and run the PARAFAC model again. The results with the reduced set of electrodes are depicted in Figure 4.

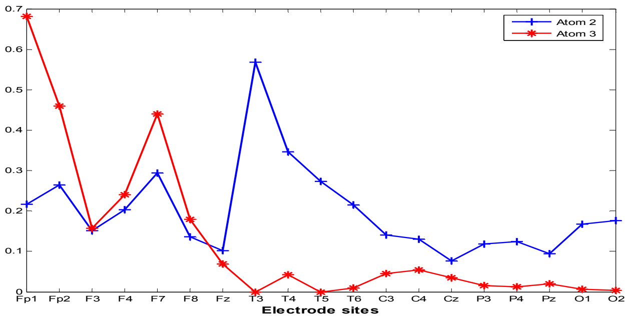

Figure 3. Participant B. Comparison of the spatial signatures corresponding to Atom 2 and Atom 3 plotted in Figure 2.

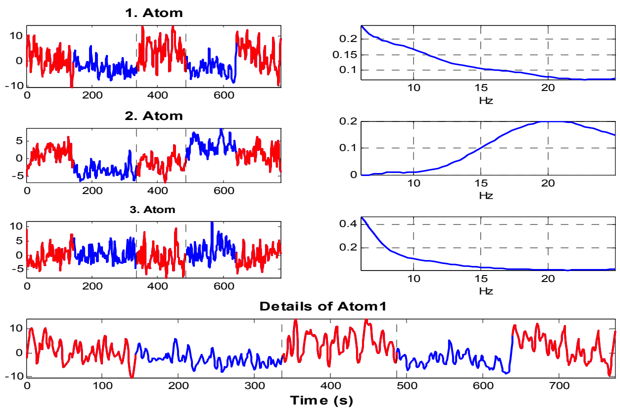

Figure 4. Loadings of the three PARAFAC atoms extracted from EEG recordings of Participant B using the reduced set of 12 electrodes. Left panel: Temporal signatures of the EEG atoms. Red marks indicate periods of high workload, blue line marks the low workload periods. Vertical dotted lines separate three distinct experimental sessions. Bottom panel: Detailed plot of the temporal loadings of Atom 2. Right panel: Spectral signatures corresponding to the atoms numbered in the left panel.

Now three distinct atoms can be observed. While the third atom seems to represent overall EEG power indicating 1/f trend, the first and the second atom seem to be two spectrally complimentary atoms which when applied together discriminate periods of low and high workload. However, although the spectral concentration of the second atom around 20 Hz and its decay at higher frequencies indicate that this atom may represent the beta component in EEG, the spatial distribution shows high influence of the frontal F3, F4 and F8 sites. Therefore the influence of movement artifact in this atom cannot be ruled out. Note that using the reduced set of electrodes increased the core consistency to 87% indicating good fit of the model to data. This is in contrast when the full set of electrodes was used and the core consistency value below 20% indicated poor fit. Similar three atoms to the ones plotted in Figure 4 were observed in Participant K, however, using the full set of electrodes. While two atoms resemble Atoms 1 and 3 in Figure 4, the third extracted atom in this participant resemble the movement atom depicted in Figure 2. This atom was spatially concentrated on Fp1, Fp2, F8 and T4 electrode sites. Removal of these sites and also additional to noise susceptible sites (F3, F4, F7, F8, T3, T5 and T6) did not change the structure of the extracted atoms, indicating that the observed movement related artifact globally influences EEG recordings at all sites.

4. CONCLUSIONS

This study has proven to be an extremely fruitful and penetrating view of an entirely new approach to multi-dimensional analysis of experiments in which EEG is used to detect changes in mental states. The results speak conclusively to the fact the atomic decomposition provides a novel view and powerful insight concerning the interactions of brain regions and oscillatory EEG sources as they change with mental states. Although the results are impressive, we feel that this project has barely scratched the surface of the potential for application of atomic decomposition to EEG.

Additional results have been obtained using atomic decomposition of coherence in mental workload and cognitive fatigue. The results with coherence measures proved to be more consistent across subjects and interpretable for workload assessment. A detailed description of these results is beyond the scope of this report, but will be presented in the corresponding conference poster. Copies of the poster presentation may be obtained in the future from the author.

Of most importance to the US Army and its need to accurately assess operator functional states, the methods we have developed here should be extended in two important directions. First, as with our prior work using PLS and linear or nonlinear classifiers, we must use atomic decomposition to extract features of EEG that serve as inputs to classifiers of mental states. Our experience with such classification work and testing will allow us to rapidly develop these methods and apply them to the existing data sets with minimal effort. Secondly, as atomic decomposition is relatively new in the analysis of EEG, we must design specific experiments that will allow us to test hypotheses concerning the validity and utility of the method in controlled studies.

For this to succeed we will seek partnerships with experimental groups and add our methodology to ongoing and planned experiments, to be as efficient as possible in the early development of the methodology. Should atomic decomposition methods prove generally valid and useful in EEG applications, we will aim to publish the fundamental advances in academic journals and distribute the underlying software technology through commercial avenues.

5. REFERENCES

[1] Wallerius, J., Trejo, L. J, Matthews, R., Rosipal, R., and Caldwell, J. A. (2005). Robust feature extraction and classification of EEG spectra for real-time classification of cognitive state. 11th International Conference on Human Computer Interaction and 1st International Conference on Augmented Cognition, July 22-27, Las Vegas, NV.

[2] Trejo, L.J., Matthews, R., & Allison, B.Z. (2007). Experimental Design and Testing of a Multimodal Cognitive Overload Classifier. In D.D. Schmorrow, D.M. Nicholson, J.M. Drexler, & L.M. Reeves (Eds.), *Foundations of Augmented Cognition,* (4th ed., pp. 13-22). Strategic Analysis, Inc., Arlington. VA.

[3] Trejo, L. J., Knuth, K., Prado, R., et al. (2007). EEG-based estimation of mental fatigue: Convergent evidence for a three-state model. In D.D. Schmorrow, L.M. Reeves (Eds.): *Augmented Cognition, HCII 2007*, LNAI 4565, pp. 201–211, 2007. Berlin: Springer-Verlag.

[4] Rosipal, R., Trejo, L.J. & Nunez, P.L. (2009). Application of Multi-way EEG Decomposition for Cognitive Workload Monitoring. In Vinzi V.E, Tenenhaus M., Guan R. (eds.), *Proceedings of the 6th International Conference on Partial Least Squares and Related Methods*, Beijing, China, pp. 145-149.

[5] Trejo, L. J., Kochavi, R., Kubitz, K., Montgomery, L. D., Rosipal, R., & Matthews, B. (2006, January). EEG-based estimation of mental fatigue. Available on line at: http://publications.neurodia.com/Trejo-et-al-EEG-Fatigue-2006-Manuscript.pdf.

[6] Gevins, A., Smith, M.E., Leong, H., McEvoy, L., Whitfield, S., Du, R., et al. (1998). Monitoring working memory load during computer-based tasks with EEG pattern recognition methods. Human Factors, 40, 79-91.

[7] Nunez, P.L., Silberstein, R.B., Carpentar, M.R., Srinivasan, R., Wijesinghe, R.S., Tucker, D.M., Cadusch, P.J. and Wu, X. (1999). EEG coherency. II: Comparisons of multiple measures of EEG coherency differences between resting and cognitive states, *Clinical Neurophysiology,* **110**, 469-486.